Progress In Electromagnetics Research B, Vol. 20, 245–262, 2010

NOVEL COMPACT DUAL-BAND BANDPASS MICROSTRIP FILTER

S. Vegesna and M. Saed

Department of Electrical and Computer Engineering
Texas Tech University
Lubbock, Texas 79409, USA

Abstract—In this paper, a novel microstrip structure is developed to realize a dual-band bandpass filter. The proposed bandpass structure uses a microstrip resonator with two independently controlled resonance frequencies producing two frequency bands of interest controlled by adjusting the dimensions of the resonator. Parametric analysis is performed on the structure to determine the optimum dimensions to obtain the desired frequency response and is explained in the paper. The dual-band bandpass filter developed in this paper exhibits dual operating frequencies at 1390 MHz and 2520 MHz with 9.85% and 9.92% fractional bandwidths respectively. We achieved a compact second-order dual-band bandpass filter with controllable resonance frequencies and low insertion losses in the passband with high selectivity. The measured results are in good agreement with simulated results. Additionally, it can be easily fabricated and can be used in applications where miniaturization and compatibility with microstrip technology are of primary concern.

1. INTRODUCTION

Recently, extensive research efforts have focused on realization of compact microwave structures for multiband wireless services and dual communication channels to reduce the circuit size and cost of the communication equipment such as dual-band antennas [1, 2], dual-band amplifiers [3] and dual-band filters [4–8, 15, 16]. In this paper, a novel dual-band bandpass filter structure is investigated which is compact in size and can be easily integrated. In general, conventional dual-band filters are designed by cascading two filter structures with different

Corresponding author: M. Saed (mohammad.saed@ttu.edu).

passbands [6]. But dual-band filters realized using this approach require two different filters and the size of these dual-band filters is comparatively large. Therefore, a single circuit with dual-band response is preferred to reduce circuit area and thereby cost. Many approaches have been previously presented for realization of integrated dual-band filters. For example, in [7] and [8] dual-band filters are designed using stepped-impedance resonators (SIRs) by utilizing the dual-band characteristics of SIRs [9]. One of the advantages of designing dual-band filters using SIRs is that the position of the dual-bands can be designed conveniently. However, it is difficult to adjust the coupling between the resonators to meet the dual-band specifications of the filter simultaneously [10]. For the dual-band filter designed using SIRs in [7], the maximal $|S_{11}|$ magnitudes over the passbands are about -10 dB and a dual-band impedance transformer has to be used in order to improve the performance. Thus, with the design method specified in [7], inclusion of an impedance transformer to improve the return loss ($|S_{11}|$) makes the circuit area larger. In [11], a fourth-order dual-band bandpass filter has been developed with equal-length split-ring resonators with two-high impedance transformers placed between the input 50 ohm lines and the SRRs to achieve better frequency response characteristics. The main advantages of filters we present in this paper include the realization of a more compact structure operating at dual frequencies that can be controlled independently, with low insertion loss ($|S_{21}| \leq 1.2$ dB) and high return loss ($|S_{11}| \geq 15$ dB) in both passbands, and without the need for impedance transformation.

The structure discussed in this paper is a modification of the conventional split-ring resonator (SRR) proposed by Pendry et al. [12] as shown in Figure 1. The outer loop in the proposed resonator is tuned at first bandpass frequency and inner loop is tuned at the second bandpass frequency and it shares the common side with the outer resonator. This novel compact structure has not been designed or discussed previously in realization of microwave filter structures. Extensive parametric analysis was performed to understand the effect of the various parameters on filter performance. All the simulations presented in this paper are done using EM software Ansoft Designer. Simulations results were verified experimentally. This paper is organized as follows. In Section 2, the design of the proposed dual-band bandpass filter is discussed. Section 3 presents a detailed parametric analysis to determine the optimum dimensions of the structure to achieve a practical filter with improved pass bandwidths and selectivity. In Section 4, experimental results of the fabricated filter prototype along with comparison of simulation and measured

frequency responses are presented. Finally, conclusions of this paper are presented in Section 5.

2. DUAL-BAND RESONATOR

The proposed microstrip resonator to realize dual-band bandpass characteristics in comparison to the conventional split-ring resonator (SRR) is shown in Figure 1. The difference between the two structures is the orientation of the inner ring and it shares the same leg or base with the outer ring in the new structure. In order to exhibit dual bandpass characteristic, the lengths of the outer ring and inner ring of the new structure are chosen such that they resonate at the two desired frequencies (say f_1 and f_2). Suppose f_1 is less than f_2, the outer resonator in Figure 1(b) is tuned to the resonance frequency f_1 and the inner resonator is tuned to the resonance frequency f_2. The resonance frequency (f_1 or f_2) depends on the length of each resonator, dielectric constant of the substrate, its thickness, and trace width.

Since the resonators are frequency selective, the rings are excited only when the signal frequency is close to the resonant frequency of the rings. At signal frequencies close to f_1, the outer resonators get excited and the signal propagates from the input port to the output port, and for frequencies close to f_2 the inner resonators propagate the signal to the output port.

In order to investigate the frequency response characteristics of the resonator shown in Figure 1(b), the outer resonator is made to resonate at 1.5 GHz and the inner resonator at 2.5 GHz. Figure 2 shows the design of the resonator and is simulated using the EM software Ansoft Designer. The dimensions of the structure shown in Figure 2 are as

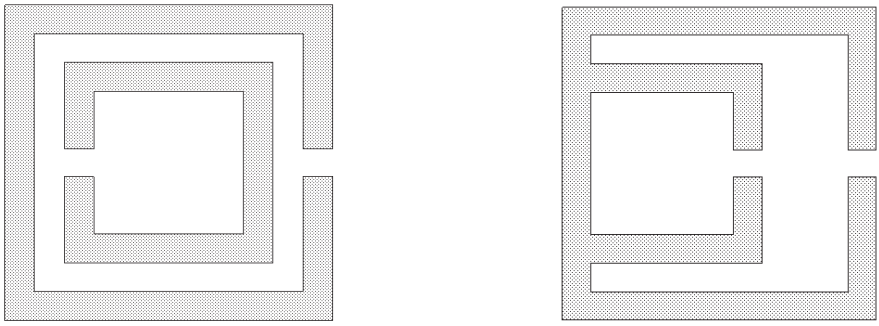

Figure 1. (a) Conventional SRR structure. (b) Proposed structure.

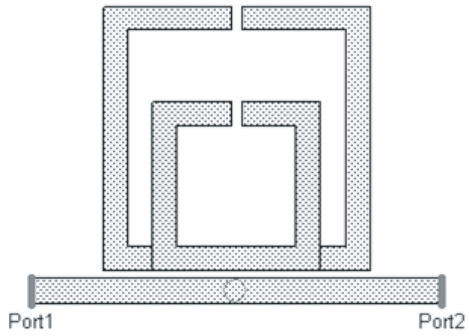

Figure 2. Unit cell structure.

follows: the length of the outer ring is 11 mm and that of the inner ring is 7 mm with trace width of 1 mm for both. The coupling space between the resonator and the feed line is 0.3 mm, side spacing between the inner and the outer rings is 1 mm, and width of the feed line is 1.192 mm for a 50 ohm characteristic impedance on Rogers RO3010 dielectric substrate ($h = 1.27$ mm and $\varepsilon_r = 10.2$).

The simulated frequency response ($|S_{11}|_{\mathrm{dB}}$ and $|S_{21}|_{\mathrm{dB}}$) of the unit cell is shown in Figure 3 and has two resonant peaks at 1.5 GHz and 2.5 GHz exhibiting a dual bandpass response confirming the dual-band bandpass response of the proposed resonator.

In order to realize a more practical filter with desired characteristics, higher order filters can be implemented using multiple coupled resonators [13]. The amount of coupling between the cascaded structures depends on various parameters such as physical dimensions of the structure, frequency of operation, spacing between the structures, and substrate properties. A second order bandpass filter using two coupled dual-band resonators is shown in Figure 4. Input and output 50 ohm microstrip feed lines are directly tapped onto the resonators.

The general design technique for realizing coupled resonator filters is done using two methods: (i) a method based on coupling coefficients of coupled resonators and the external quality factors of the input and output resonators, and (ii) a method using parametric analysis embedded in EM software capable of full-wave analysis. The first method of determining optimum parameters is explained in detail in [14]. In this paper, to simplify the analysis for a dual bandpass structure, we chose the parametric analysis method for determining optimum dimensions of the structure as explained in the next section.

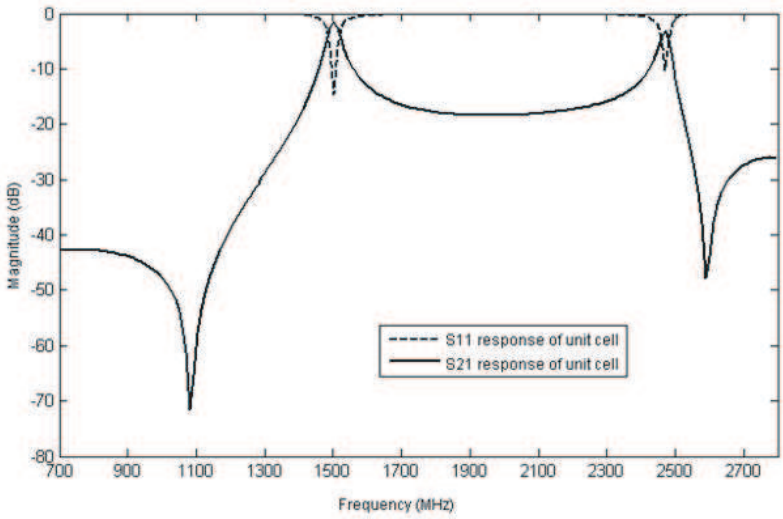

Figure 3. Simulated frequency response of the unit cell.

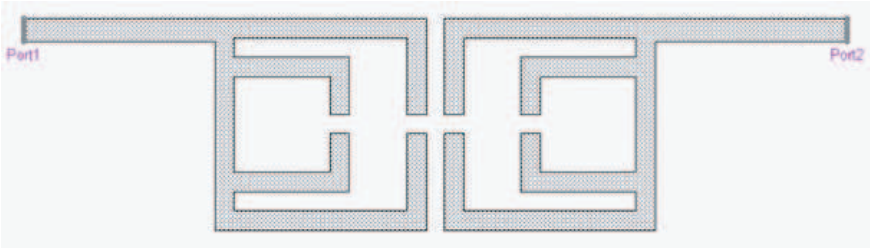

Figure 4. Basic structure of two coupled resonators.

3. PARAMETRIC ANALYSIS

This section describes the effect of various parameters on the frequency of resonance and how optimum dimensions for the structure are determined. The parameters that control the frequency response characteristics of the structure are labeled in Figure 5. Initially, the length of the outer ring (L_1) is 11 mm, length of the inner ring (L_2) is 7 mm, width of the resonator arms (w) is equal to 1 mm, the coupling space (s) between the adjacent resonators is chosen is to be 1 mm, input and output feed lines are directly tapped on to the resonators without any offset and the dimensions of the other parameters are g_1 = 1.5 mm, g_2 = 0.5 mm, s_1 = 1 mm and s_2 = 3 mm.

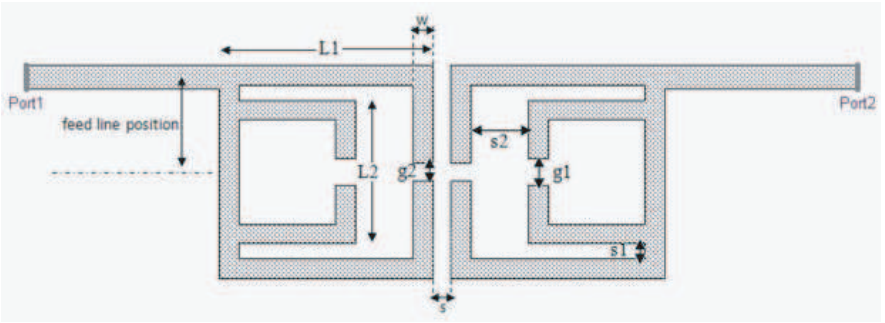

Figure 5. Parameters that control the frequency response of this structure.

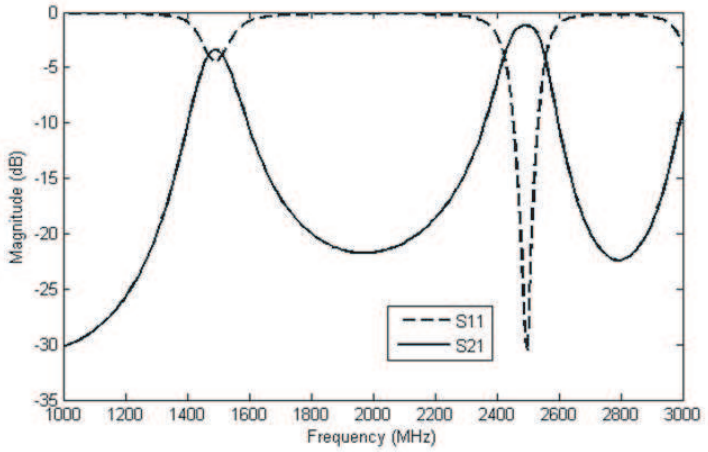

Figure 6. Simulated frequency response of the coupled structure with dimensions in mm: $L_1 = 11$, $L_2 = 7$, $w = 1$, $s = 1$, feed line position $= 0$, $g_1 = 1.5$, $g_2 = 0.5$, $s_1 = 1$, $s_2 = 3$.

The simulated frequency response of the structure shown in Figure 5 with the initial dimensions mentioned above is shown in Figure 6. Parametric analysis is performed with various combinations of width (w), coupling spacing between the resonators (s), offset position of the input/output feed lines, and gaps (g_1, g_2). Since it is difficult to show the analysis of all the parameters in this paper, only selected results to help understand how these parameters affect the frequency response are presented.

From the frequency response in Figure 6, we observe that the insertion loss ($|S_{21}|_{\text{dB}} = 4\,\text{dB}$) and return loss ($|S_{11}|_{\text{dB}} = 4.5\,\text{dB}$) in the first passband (f_1) are not good enough for the structure with the initial dimensions. For the second band, the insertion loss ($|S_{21}|_{\text{dB}} = 1.2$ dB) and return loss ($|S_{11}|_{\text{dB}} = 30$ dB) are acceptable. Parametric analysis is performed in order to determine the optimum dimensions so that low insertion loss and high return loss are obtained in both frequency bands. The following describes the effect of the various parameters.

3.1. Position of Input Feed Line

The position of the feed line tapped onto the resonator can be changed to adjust the return loss or the insertion loss. Figure 7 shows the structure with an offset to input feed line. For analyzing the effect

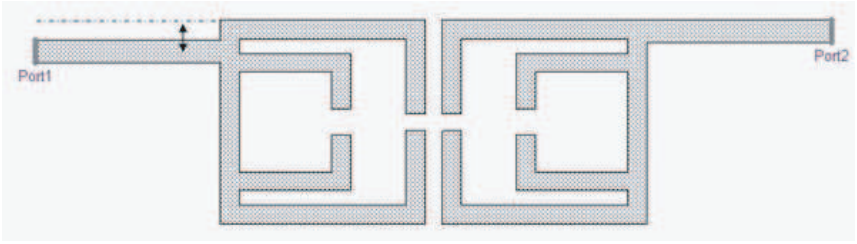

Figure 7. Varying the input feed line position.

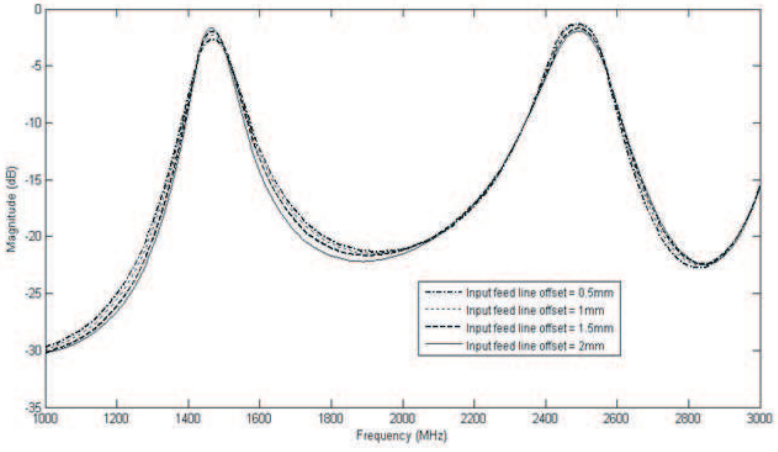

Figure 8. S_{21} frequency response for different input feed line offset.

of the feed line on the frequency response, the position of the input feed line is varied, while all the other parameters are kept constant ($L_1 = 11\,\text{mm}$, $L_2 = 7\,\text{mm}$, $w = 1\text{mm}$, $s = 1\,\text{mm}$, $g_1 = 1.5\,\text{mm}$, $g_2 = 0.5\,\text{mm}$, $s_1 = 1\,\text{mm}$ and $s_2 = 3\,\text{mm}$). Figures 8 and 9 show the effect of varying the position of the input feed line on S_{21} and S_{11} frequency response, respectively.

It can be observed from Figure 8 and Figure 9 that the position of the feed line has more pronounced impact on S_{11} frequency response rather than on S_{21} frequency response. The S_{11} frequency response can be improved in one band by properly choosing the input feed line position. However, improving S_{11} in one band using input feed line offset causes S_{11} in the other band to deteriorate. Varying the offset of both input and output feed lines did not help either. The frequency responses $|S_{21}|_{\text{dB}}$ and $|S_{11}|_{\text{dB}}$ for various positions of the input and output feed lines are shown in Figures 10 and 11 with the dimensions of the other parameters kept constant ($L_1 = 11\,\text{mm}$, $L_2 = 7\,\text{mm}$, $w = 1\,\text{mm}$, $s = 1\,\text{mm}$, $g_1 = 1.5\,\text{mm}$, $g_2 = 0.5\,\text{mm}$, $s_1 = 1\,\text{mm}$ and $s_2 = 3\,\text{mm}$).

Varying the position of the feed lines only is not enough to obtain satisfactory responses in both bands simultaneously. Next, we consider varying the gaps g_1 and g_2 (with no feed line offsets).

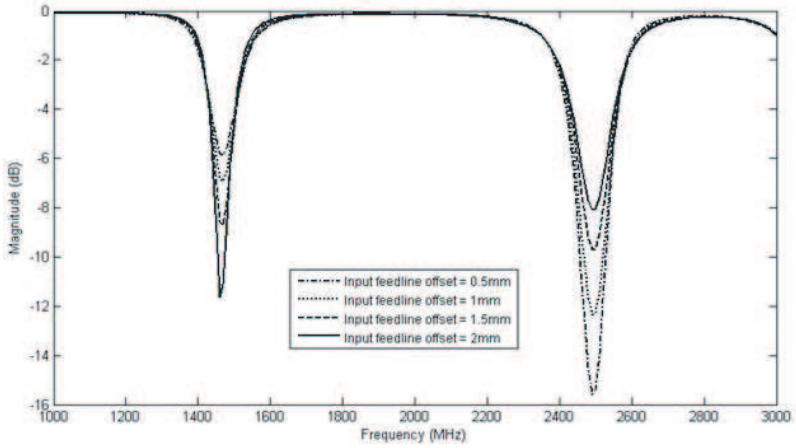

Figure 9. S_{11} frequency response for different input feed line offsets.

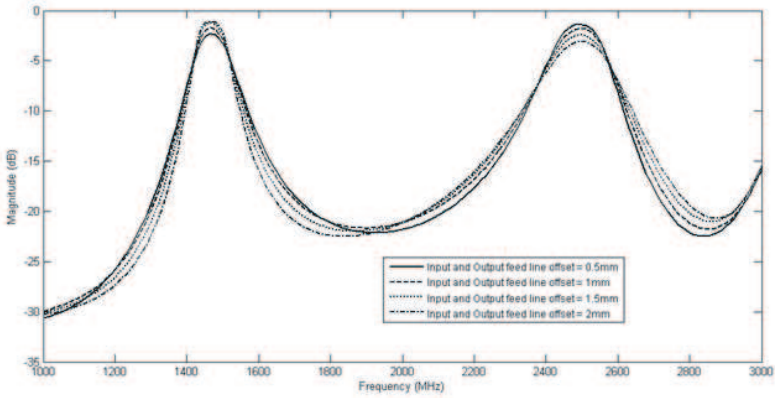

Figure 10. $|S_{21}|_{\mathrm{dB}}$ when both input and output feed lines are offset.

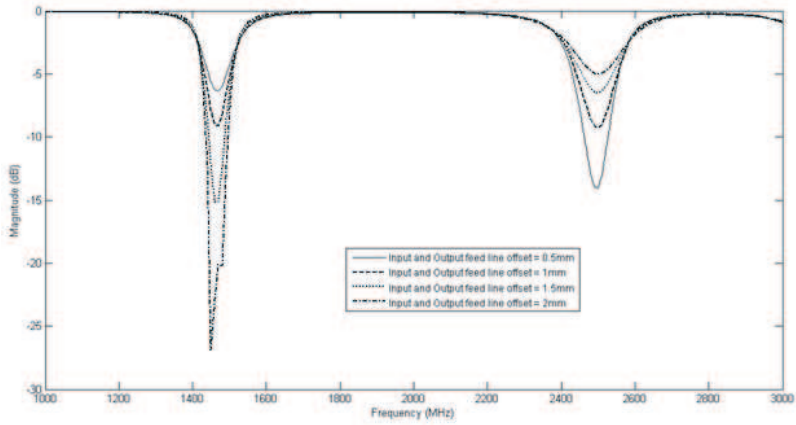

Figure 11. $|S_{11}|_{\mathrm{dB}}$ when both input and output feed lines are offset.

3.2. Gap Widths g_1 and g_2

The effect of the parameters g_1 and g_2 is analyzed with no offset to the feed line position; the dimensions of the other parameters are kept constant ($L_1 = 11\,\mathrm{mm}$, $L_2 = 7\,\mathrm{mm}$, $w = 1\,\mathrm{mm}$, $s = 1\,\mathrm{mm}$, feed line position $= 0\,\mathrm{mm}$ (no offset), $s_1 = 1\,\mathrm{mm}$ and $s_2 = 3\,\mathrm{mm}$). The simulated frequency responses ($|S_{21}|_{\mathrm{dB}}$ and $|S_{11}|_{\mathrm{dB}}$) for selected values of g_1 and g_2 are shown in Figure 12 and Figure 13.

It can be concluded from the analysis done on the parameters g_1 and g_2 that small variations of these parameters do not affect

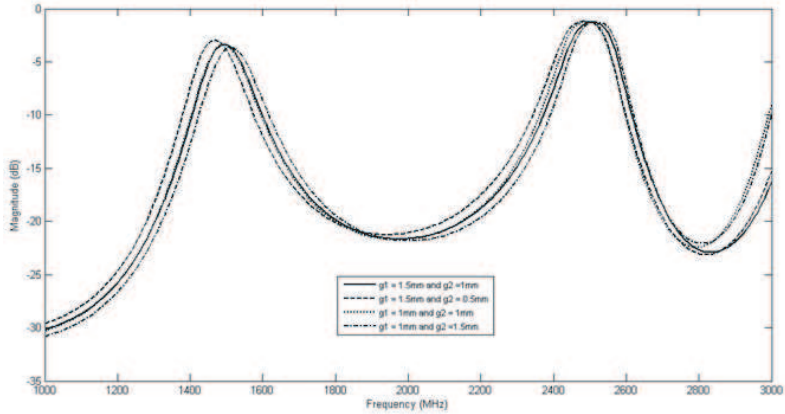

Figure 12. Simulated $|S_{21}|_{\mathrm{dB}}$ frequency response for different values of g_1 and g_2.

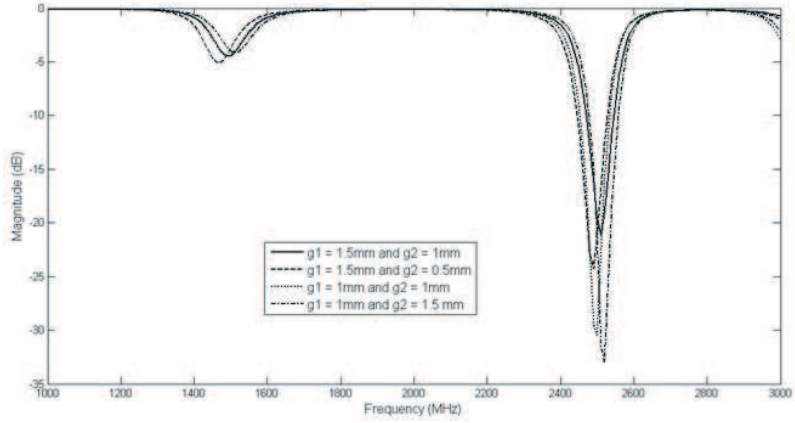

Figure 13. Simulated S_{11} frequency response for different values of g_1 and g_2.

the frequency response characteristics significantly for the structure discussed. Since, neither tuning the feed line position nor the gap (g_1 or g_2) improve the S_{11} frequency response at the first operating frequency, the values used for these parameters are the initial values.

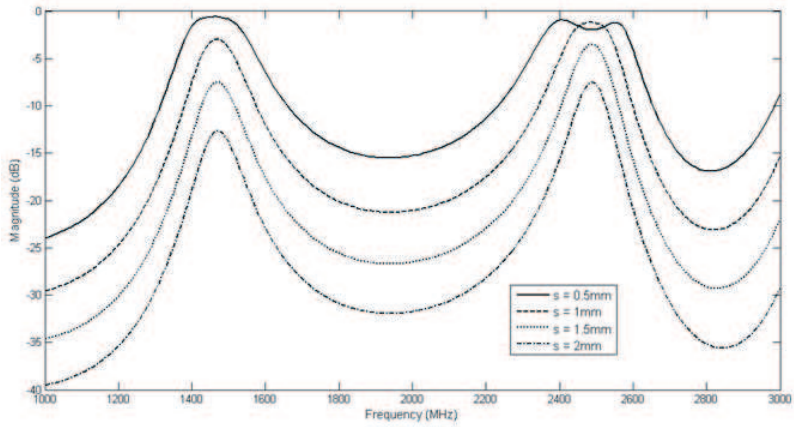

Figure 14. $|S_{21}|_{\mathrm{dB}}$ frequency response for various spacing values.

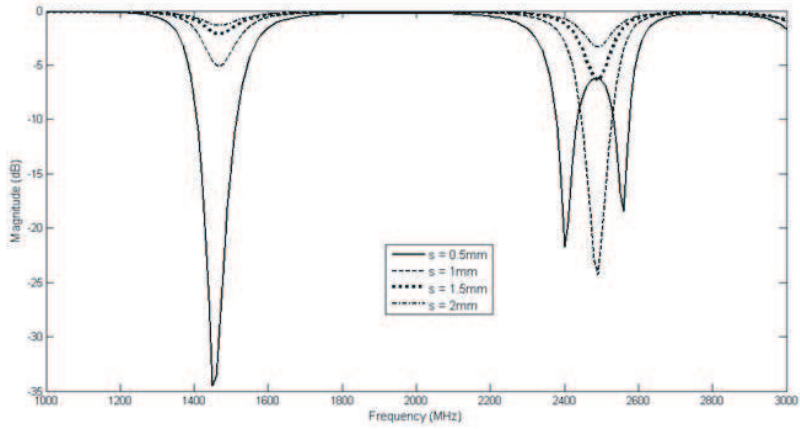

Figure 15. $|S_{11}|_{\mathrm{dB}}$ frequency response for various spacing values.

3.3. Coupling Space(s) between the Resonators

The spacing between the adjacent resonators controls the coupling between the resonators in order to obtain a desired response and bandwidth in the passband region. The spacing between the resonators is varied while the remaining parameters are kept constant. The dimensions of the other parameters are as follows. $w = 1\,\mathrm{mm}$, feed line position $= 0\,\mathrm{mm}$ (no offset) $g_1 = 1.5\,\mathrm{mm}$, $g_2 = 0.5\,\mathrm{mm}$, $s_1 = 1\,\mathrm{mm}$ and $s_2 = 3\,\mathrm{mm}$. The frequency responses ($|S_{11}|_{\mathrm{dB}}$ and $|S_{21}|_{\mathrm{dB}}$) of the structure for different values of spacing between the resonators are shown in Figure 14 and Figure 15.

From the S_{21} frequency response (Figure 14), we observe that as the spacing between the resonators is increased, insertion loss also increases and passband bandwidth decreases. From the S_{11} frequency response (Figure 15), the return loss increases with coupling space. The coupling space between the resonators is an important parameter that controls the insertion loss, return loss, and passband bandwidth without shifting the resonance frequencies. Better return loss ($>$ 20 dB) is obtained in the first passband region while the maximum return loss in the second passband is not good enough ($>$7 dB) for a spacing between the resonators of 0.5 mm. The insertion loss for this spacing value is less than 1.5 dB for both frequency bands. Since the filter performance has improved with a spacing of 0.5 mm, except for somewhat low maximum return loss in the second band, we fixed the spacing to this value for the next optimization step.

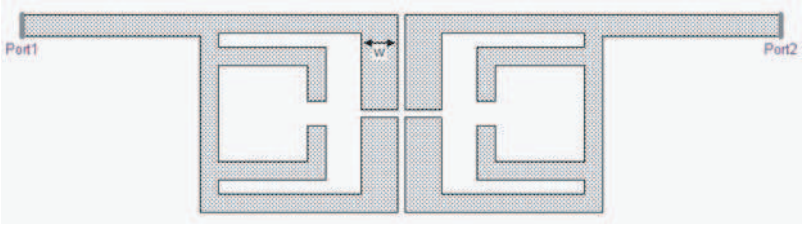

Figure 16. Variation of width of the outer edge.

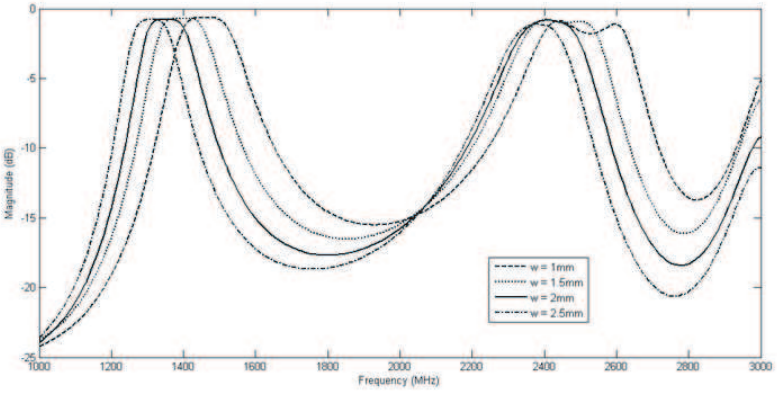

Figure 17. $|S_{21}|_{\mathrm{dB}}$ frequency response for various widths.

3.4. Width of the Outer Edge (w)

As mentioned earlier, only the return loss in the second needs improvement. Since varying the trace width of the entire resonator drastically affects the center frequencies of both bands as well as the frequency responses, we decided to vary only the width of the outer edge of the resonator since it is easier and achieves the desired responses, as shown in Figure 16. The width was changed from 1 mm to 2.5 mm using a step of 0.5 mm. The trace width for the rest of the resonator was kept at 1 mm and the other parameters were kept as before ($L_1 = 11$ mm, $L_2 = 7$ mm, $s = 0.5$ mm, feed line position $= 0$ mm, $g_1 = 1.5$ mm, $g_2 = 0.5$ mm).

The frequency responses ($|S_{11}|_{\mathrm{dB}}$ and $|S_{21}|_{\mathrm{dB}}$) are shown in Figure 17 and Figure 18. Changing the width w causes a shift in the center frequencies of the two bands and affects the insertion loss and return loss. Table 1 summarizes the return loss values at the center frequencies of both bands for different widths. Both bands have very good return loss and insertion loss for a width $w = 2$ mm. The return

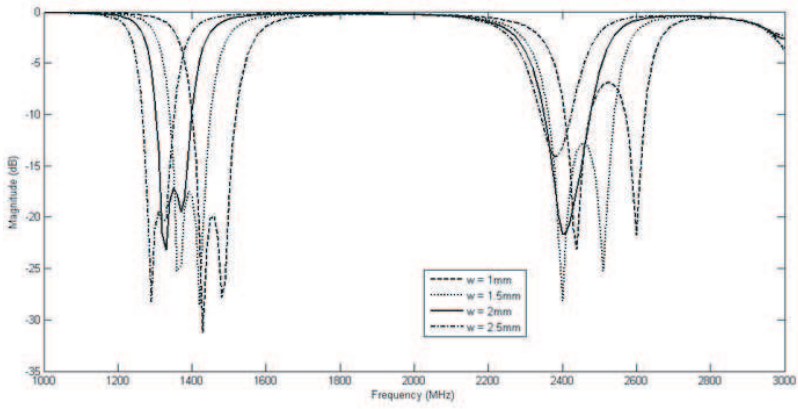

Figure 18. $|S_{11}|_{\mathrm{dB}}$ frequency response for various widths.

Table 1. S_{11} frequency response for various widths.

	S_{11}, Resonant freq f_1	S_{11}, Resonant freq f_2
W (1 mm)	−20 dB, 1460 MHz	−7 dB, 2520 MHz
W (1.5 mm)	−17 dB, 1390 MHz	−12 dB, 2450 MHz
W (2 mm)	−17 dB, 1350 MHz	−21 dB, 2410 MHz
W (2.5 mm)	−19 dB, 1310 MHz	−13 dB, 2390 MHz

loss at the center frequency of the first band is 17 dB, and it is 21 dB for the second band. The insertion loss for both frequencies is less than 1 dB for $w = 2$ mm.

The final parameters for the optimized filter are: $L_1 = 11$ mm, $L_2 = 7$ mm, width of the outer edge $w = 2$ mm, coupling spacing $s = 0.5$ mm, feed line position = 0 mm (no offset) $g_1 = 1.5$ mm, $g_2 = 0.5$ mm, $s_1 = 1$ mm and $s_2 = 2$ mm. The frequency responses of the optimized filter ($|S_{11}|_{\text{dB}}$ and $|S_{21}|_{\text{dB}}$) are shown in Figure 19. From the figures, the return loss is around 17 dB at 1350 MHz (f_1) and 21 dB at 2410 MHz (f_2); the insertion loss is around 0.7 dB at 1350 MHz and 0.9 dB at 2410 MHz.

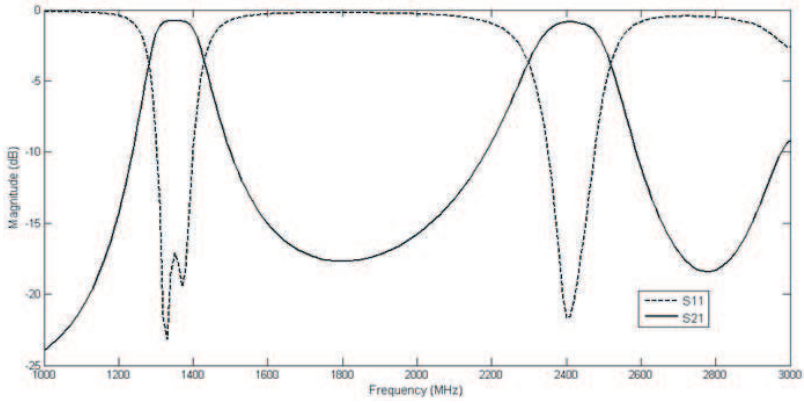

Figure 19. Simulated frequency response of the optimized filter.

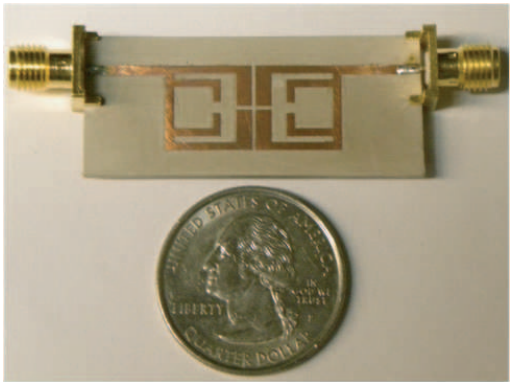

Figure 20. Photograph of the fabricated filter.

4. EXPERIMENTAL RESULTS

The optimized dimensions of the filter determined using the parametric analysis were used to fabricate a filter prototype on a Duroid substrate RO3010 (10.2 and thickness $h = 1.27\,\text{mm}$) to verify the performance

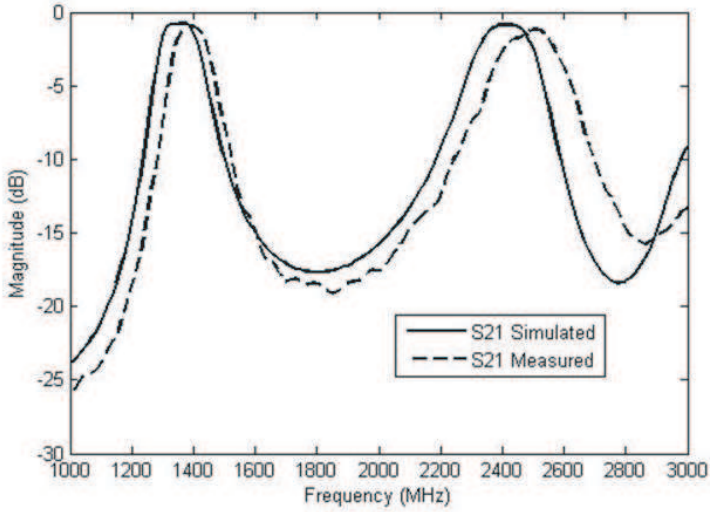

Figure 21. Measured and simulated $|S_{21}|_{\text{dB}}$ frequency response.

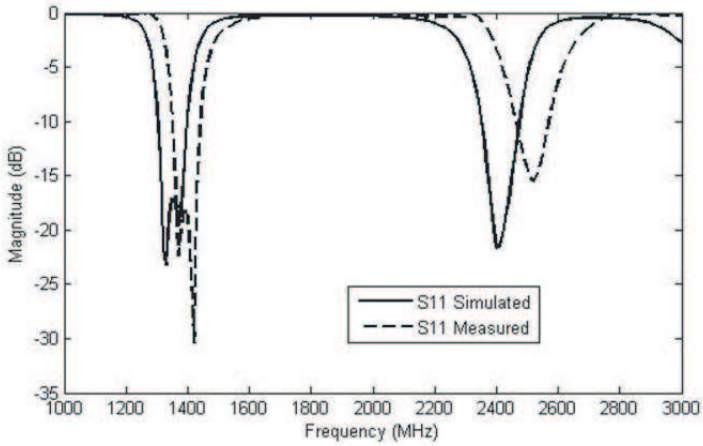

Figure 22. Measured and simulated $|S_{11}|_{\text{dB}}$ frequency response.

Table 2. Characteristics of the fabricated dual-band bandpass filter.

	Center frequency *first passband*, $f_1 = 1390\,\text{MHz}$	Center frequency *second passband*, $f_2 = 2520\,\text{MHz}$
Insertion loss	$-0.96\,\text{dB}$	$-1.2\,\text{dB}$
Return loss	$-18\,\text{dB}$	$-15.5\,\text{dB}$
Fractional bandwidth	9.85 %	9.92%

of the proposed new dual bandpass filter. Fabrication is done using milling machine. The results are measured using a HP 8753C network analyzer. A photograph of the fabricated filter is shown in Figure 20. The comparison between the simulated and measured S_{11} and S_{21} frequency responses are shown in Figure 21 and Figure 22, respectively.

From Figure 21 and Figure 22, we observe that there is slight frequency shift between the measured and simulated frequency responses. This is mostly due to the somewhat crude fabrication process which used a milling machine. The measured frequency responses show excellent return loss and insertion loss in both bands. Table 2 summarizes the performance of the fabricated filter.

5. CONCLUSIONS

A new compact dual-band bandpass filter has been successfully realized with measured dual operating frequencies at 1390 MHz and 2520 MHz with insertion losses less than 1.2 dB and return losses greater than 15 dB. The influence of the geometric parameters of the structure on the frequency response characteristics of the structure were investigated using parametric analysis in a commercial EM software. A filter prototype was fabricated using the optimized dimensions obtained. A milling machine used to fabricate the prototype filter. Experimental measurements and theoretical simulations of the filter showed excellent return loss and insertion loss in both frequency bands. The small shift between simulated and measured responses is attributed mainly to the crude fabrication process used. Higher order filters can be easily designed using the dual-band resonator investigated in this paper using cascaded resonators or cross coupled configurations.

REFERENCES

1. Kuo, Y. L. and K. L. Wong, "Printed double-T monopole antenna for 2.4/5.2 GHz dual-band WLAN operations," *IEEE Trans. Antennas Propagat.*, Vol. 51, No. 9, 2187–2192, Sep. 2003.
2. Llorens, D., P. Otero, and C. Camacho-Penalosa, "Dual-band, single CPW port, planar-slot antenna," *IEEE Trans. Antennas Propagat.*, Vol. 51, No. 1, 137–139, Jan. 2003.
3. Hashemi, H. and A. Hajimiri, "Concurrent multiband low-noise amplifiers theory, design and applications," *IEEE Trans. Microw. Theory Tech.*, Vol. 50, No. 1, 288–301, Jan. 2002.
4. Tsai, L. C. and C. W. Hsue, "Dual-band bandpass filters using equal length coupled serial-shunted lines and Z-transform technique," *IEEE Trans. Microw. Theory Tech.*, Vol. 52, No. 4, 1111–1117, Apr. 2004.
5. Kuo, J.-T. and H.-S. Cheng, "Design of quasi-elliptic function filters with a dual-passband response," *IEEE Microw. Compon. Lett.*, Vol. 14, No. 10, 472–474, Oct. 2004.
6. Miyake, H., S. Kitazawa, T. Ishizaki, T. Yamada, and Y. Nagatomi, "A miniaturized monolithic dual band filter using ceramic lamination technique for dual mode portable telephones," *1997 IEEE MTT-S Int. Microwave Symp. Dig.*, 789–792, 1997.
7. Kuo, J.-T., T.-H. Yeh, and C.-C. Yeh, "Design of Microstrip Bandpass Filters with a Dual-passband response," *IEEE Trans. Microwave Theory and Tech.*, Vol. 53, No. 4, 1331–1337, Apr. 2005.
8. Chang, S.-F., J.-L. Chen, and S.-C. Chang, "New dual-band bandpass filters with step-impedance resonators in comb and hairpin structures," *Asia-Pacific Microwave Conf.*, 793–796, 2003.
9. Quendo, C., E. Rius, and C. Person, "An original topology of dual-band filter with transmission zeros," *2003 IEEE MTT-S Int. Microwave Symp. Dig.*, 1093–1096, 2003.
10. Guan, X., Z. Ma, P. Cai, Y. Kobayashi, T. Anada, and G. Hagiwara, "Synthesis of dual-band bandpass filters using successive frequency transformations and circuit conversions," *IEEE Microwave and Wireless Components Letters*, Vol. 16, No. 3, Mar. 2006.
11. Garcia-Lamperez, A. and M. Salazar-Palmat, "Dual band filter with split-ring resonators," *Microwave Symposium Digest, 2006. IEEE MTT-S International*, 519–522, Jun. 2006.
12. Pendry, J. B., A. J. Holden, D. J. Robbins, and W. J. Stewart, "Magnetism from conductors and enhanced nonlinear phenom-

ena," *IEEE Trans. Microwave Theory Tech.*, Vol. 47, 2075–2084, 1999.

13. Marques, R., F. Martin, and M. Sorolla, *Metamaterials with Negative Parameters, Theory, Design and Microwave Applications*, John Wiley & Sons, Inc., New Jersey, 2008.
14. Hong, J.-S. and M. J. Lancaster, "Couplings of microstrip square open-loop resonators for cross-coupled planar microwave filters," *IEEE Trans. Microwave Theory Tech.*, Vol. 44, 2099–2109, Dec. 1996.
15. Wang, X.-H., B.-Z. Wang, and K. J. Chen, "Compact broadband dual-band bandpass filters using slotted ground structures," *Progress In Electromagnetics Research*, PIER 82, 151–166, 2008.
16. Wu, G.-L., W. Mu, X.-W. Dai, and Y.-C. Jiao, "Design of novel dual-band bandpass filter with microstrip meander-loop resonator and CSRR DGS," *Progress In Electromagnetics Research*, PIER 78, 17–24, 2008.